

## Main-Group Compounds

International Edition: DOI: 10.1002/anie.201909144  
German Edition: DOI: 10.1002/ange.201909144

## Crystalline Divinyldiarsene Radical Cations and Dications

Mahendra K. Sharma, Sebastian Blomeyer, Beate Neumann, Hans-Georg Stammler, Maurice van Gastel, Alexander Hinz, and Rajendra S. Ghadwal\*

Dedicated to Professor Lothar Weber on the occasion of his 75th birthday

**Abstract:** The divinyldiarsene radical cations  $[(\text{NHC})\text{C}(\text{Ph})\text{As}]_2(\text{GaCl}_4)$  ( $\text{NHC} = \text{IPr}$ :  $\text{C}\{(\text{NDipp})\text{CH}_2\}_2$  **3**;  $\text{SIPr}$ :  $\text{C}\{(\text{NDipp})\text{CH}_2\}_2$  **4**;  $\text{Dipp} = 2,6\text{-}i\text{Pr}_2\text{C}_6\text{H}_3$ ) and dications  $[(\text{NHC})\text{C}(\text{Ph})\text{As}]_2(\text{GaCl}_4)_2$  ( $\text{NHC} = \text{IPr}$  **5**;  $\text{SIPr}$  **6**) are readily accessible as crystalline solids on sequential one-electron oxidation of the corresponding divinyldiarsenes  $[(\text{NHC})\text{C}(\text{Ph})\text{As}]_2$  ( $\text{NHC} = \text{IPr}$  **1**;  $\text{SIPr}$  **2**) with  $\text{GaCl}_3$ . Compounds **3–6** have been characterized by X-ray diffraction, cyclic voltammetry, EPR/NMR spectroscopy, and UV/vis absorption spectroscopy as well as DFT calculations. The sequential removal of one electron from the HOMO, that is mainly the As–As  $\pi$ -bond, of **1** and **2** leads to successive elongation of the As=As bond and contraction of the C–As bonds from **1/2**  $\rightarrow$  **3/4**  $\rightarrow$  **5/6**. The UV/vis spectrum of **3** and **4** each exhibits a strong absorption in the visible region associated with SOMO-related transitions. The EPR spectrum of **3** and **4** each shows a broadened septet owing to coupling of the unpaired electron with two  $^{75}\text{As}$  ( $I = 3/2$ ) nuclei.

Stable radicals are appealing synthetic targets in main-group chemistry<sup>[1]</sup> because they challenge conventional bonding paradigms as well as exhibit intriguing electronic structure and physical properties. Among the heavier Group 15 elements (P, As, Sb, Bi), numerous phosphorus-centered stable radicals<sup>[2]</sup> have been isolated and structurally characterized.

However, the number of crystallographically characterized arsenic,<sup>[2g,k,p,3]</sup> antimony,<sup>[4]</sup> and bismuth<sup>[5]</sup> radicals remained limited.

In 2013, Robinson et al. reported the first stable arsenic radical cation **I** (Figure 1)<sup>[3a]</sup> by one-electron oxidation of an N-heterocyclic carbene (NHC)-stabilized diatomic arsenic compound  $(\text{IPr})_2\text{As}_2$ .<sup>[6]</sup> Grützmacher and co-workers

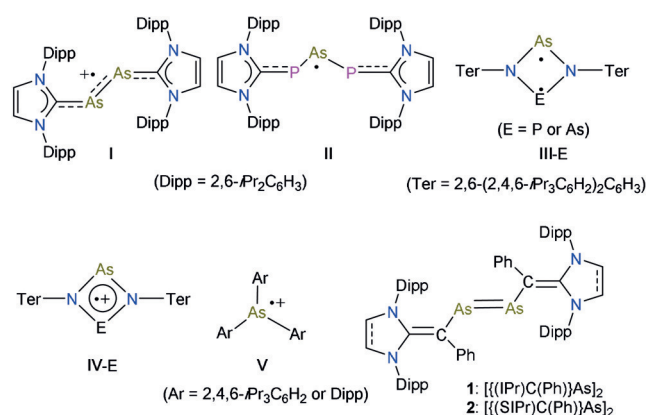


**Figure 1.** Structurally characterized arsenic-centered radicals I–V and divinyldiarsenes **1** and **2**.

reported the neutral radical **II** containing NHC-phosphinidene substituents.<sup>[2k]</sup> Schulz et al. isolated singlet diradicaloids **III-E** ( $\text{E} = \text{P}$  or  $\text{As}$ ) featuring a  $6\pi$ -electron four-membered  $\text{N}_2\text{E}_2$  ring with a considerable open-shell character.<sup>[2g,3b]</sup> Consequently, **III-E** undergo one-electron oxidation to afford the  $5\pi$ -electron radical cations **IV-E**.<sup>[2p]</sup> Very recently, Wang and co-workers reported the radical cations  $\text{Ar}_2\text{As}^{\bullet+}$  (**V**) ( $\text{Ar} = i\text{Pr}_2\text{C}_6\text{H}_3$  or  $i\text{Pr}_2\text{C}_6\text{H}_3$ ).<sup>[7]</sup> The high-lying HOMO of **III-E** and  $\text{Ar}_2\text{As}$  facilitates one-electron oxidation giving rise to radical cations **IV-E** and **V**, respectively. We recently reported crystalline divinyldiarsenes **1** and **2** derived from classical NHCs, which exhibit remarkably small HOMO–LUMO energy gap of 3.86 eV and 4.24 eV, respectively.<sup>[8]</sup> The high-lying HOMO of **1** (–4.42 eV) and **2** (–5.28 eV) encouraged us to probe the synthetic viability of corresponding stable radical cations on one-electron oxidation of **1** and **2**. Herein, we report the synthesis of crystalline divinyldiarsene radical cations  $[(\text{NHC})\text{C}(\text{Ph})\text{As}]_2(\text{GaCl}_4)$  ( $\text{NHC} = \text{IPr}$ :  $\text{C}\{(\text{NDipp})\text{CH}_2\}_2$  **3**;  $\text{SIPr}$ :  $\text{C}\{(\text{NDipp})\text{CH}_2\}_2$  **4**;  $\text{Dipp} = 2,6\text{-}i\text{Pr}_2\text{C}_6\text{H}_3$ ) as well as dications  $[(\text{NHC})\text{C}(\text{Ph})\text{As}]_2(\text{GaCl}_4)_2$  ( $\text{NHC} = \text{IPr}$  **5**;  $\text{SIPr}$  **6**).

[\*] Dr. M. K. Sharma, Dr. S. Blomeyer, B. Neumann, Dr. H.-G. Stammler, Priv.-Doz. Dr. R. S. Ghadwal  
Anorganische Molekülchemie und Katalyse, Lehrstuhl für Anorganische Chemie und Strukturchemie, Centrum für Molekulare Materialien, Fakultät für Chemie, Universität Bielefeld  
Universitätsstr. 25, 33615, Bielefeld (Germany)  
E-mail: rghadwal@uni-bielefeld.de  
Homepage: <http://www.ghadwalgroup.de>

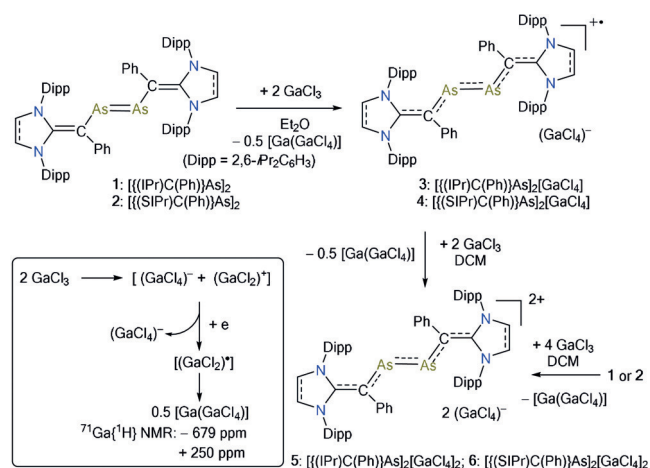
Dr. M. van Gastel  
Max-Planck-Institut für Kohlenforschung, Molecular Theory and Spectroscopy  
Kaiser-Wilhelm-Platz 1, Mülheim an der Ruhr, 45470 (Germany)

Dr. A. Hinz  
Institute of Inorganic Chemistry  
Karlsruhe Institute of Technology (KIT)  
Engesserstr. 15, 76131 Karlsruhe (Germany)

Supporting information and the ORCID identification number(s) for the author(s) of this article can be found under:  
<https://doi.org/10.1002/anie.201909144>.

© 2019 The Authors. Published by Wiley-VCH Verlag GmbH & Co. KGaA. This is an open access article under the terms of the Creative Commons Attribution License, which permits use, distribution and reproduction in any medium, provided the original work is properly cited.

We commenced our studies with electrochemical analyses of **1** and **2** (see the Supporting Information). The cyclic voltammograms (CVs) of **1** and **2** exhibit two one-electron redox events (**1**:  $-1.00$ ,  $-0.67$ ; **2**:  $-0.92$ ,  $-0.51$  V), which may be tentatively assigned to the related radical cations (**1** or **2**)<sup>•+</sup> and dications (**1** or **2**)<sup>2+</sup>, respectively (Supporting Information, Figure F1 and Table T5). One additional wave at  $-1.28$  V was observed for **1** and is most likely associated with the reduction to the corresponding radical anion. However, this wave is absent in the CV of **2**. Accordingly, treatment of an Et<sub>2</sub>O solution of **1** (green) and **2** (violet) each with two equivalents of GaCl<sub>3</sub> immediately led to the precipitation of a dark green solid. After workup, the radical cations **3** and **4** were isolated as green crystalline solids (Scheme 1). The use of an excess GaCl<sub>3</sub> should be avoided as it leads to the over oxidized products, the dications **5** and **6**. Indeed, reactions of **3** and **4** with two equivalents of GaCl<sub>3</sub> quantitatively gave **5** and **6**, respectively. Alternatively, **5** and **6** are also accessible in one-pot reaction of **1** or **2** with four equivalents of GaCl<sub>3</sub>.



**Scheme 1.** Synthesis of divinyldiarsene radical cations **3** and **4** as well as dications **5** and **6**. Reduction of GaCl<sub>3</sub> into [Ga(GaCl<sub>4</sub>)] (inset) via disproportionation of the putative GaCl<sub>2</sub> intermediate.

Two molecules of GaCl<sub>3</sub> are required for one-electron oxidation of **1** and **2**. The putative oxidizing species is (GaCl<sub>2</sub>)<sup>+</sup> that is formed according to  $2 \text{ GaCl}_3 \rightleftharpoons (\text{GaCl}_4)^- + (\text{GaCl}_2)^+$ . The reduction of (GaCl<sub>2</sub>)<sup>+</sup> yields GaCl<sub>2</sub>, which eventually disproportionates to form the stable mixed-valence Ga<sup>I</sup>/Ga<sup>III</sup> compound [Ga(GaCl<sub>4</sub>)] (Supporting Information).<sup>[9]</sup> Compounds **3–6** are stable under an inert gas atmosphere but readily decompose when exposed to air. Compound **3** and **4** were NMR-silent, thus indicating their paramagnetic nature. The dications **5** and **6** are red crystalline solids and exhibit well-resolved <sup>1</sup>H and <sup>13</sup>C{<sup>1</sup>H} NMR signals for the N-heterocyclic vinyl (NHV) moieties (Supporting Information).

Solid-state molecular structures of **3** (Figure 2), **4** (Figure 3), **5** (Figure 4), and **6** (Supporting Information, Figure F8) were determined by X-ray diffraction, which exhibit the intact As–As bond with *trans*-bent geometries along the two-coordinated arsenic atoms. The HOMO of diarsenes **1** and **2** is the  $\pi$ -orbital of the As=As bond.<sup>[8]</sup> Thus,

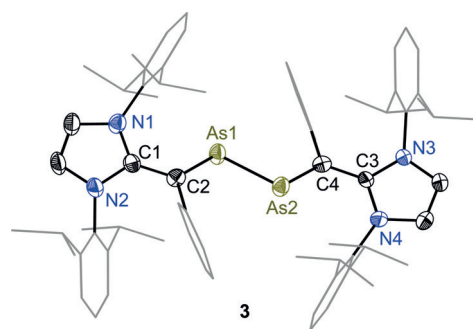


**Figure 2.** Molecular structure of divinyldiarsene radical cation **3** determined at 100 K. Ellipsoids are set at 50% probability. Hydrogen atoms, solvent molecules, and the counterion (GaCl<sub>4</sub>) are omitted for clarity.<sup>[12]</sup>

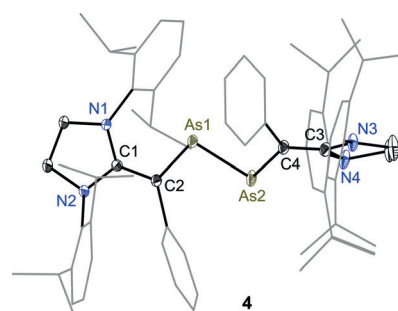


**Figure 3.** Molecular structure of divinyldiarsene radical cation **4** determined at 100 K. Ellipsoids are set at 50% probability. Hydrogen atoms, solvent molecules, minor occupied disordered atoms, and the counterion (GaCl<sub>4</sub>) are omitted for clarity.<sup>[12]</sup>

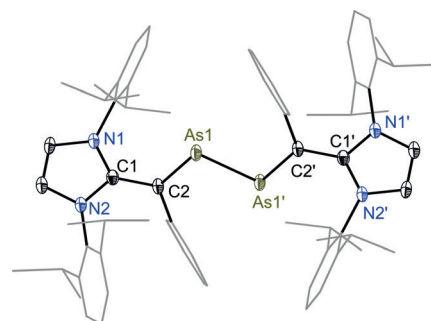


**Figure 4.** Molecular structure of divinyldiarsene dication **5** determined at 100 K. Ellipsoids are set at 50% probability. Hydrogen atoms, solvent molecules, and the counterions (GaCl<sub>4</sub>) are omitted for clarity.<sup>[12]</sup>

the formation of **3** and **4** as well as **5** and **6** is the result of sequential one electron removal from the HOMO of **1** and **2**. Clearly, this leads to a steady increase in the As–As bond length of **3** (2.322(1) Å) and **5** (2.419(1) Å) as well as **4** (2.330(1) Å) and **6** (2.414(1) Å) with respect to those of **1** (2.296(1) Å) and **2** (2.290(1) Å) (Table 1). The C2–As1/C4–As2 bond lengths of **3** (1.867(4) Å) and **4** (av. 1.876(2) Å) are shorter compared to that of **1** (1.919(1) Å) and **2** (1.936(3) Å) respectively. The C1–C2/C3–C4 bond lengths of **3** (1.424(5) Å) and **4** (av. 1.420(2) Å) are however rather stretched with respect to those of **1** (1.376(2) Å) and **2** (1.369(3) Å).

**Table 1:** Selected bond lengths [Å] and angles [°] of diarsenes (**1**, **2**) and the corresponding radical cations (**3**, **4**) and dications (**5**, **6**).

	As–As <sup>[a]</sup>	C2–As1 C4–As2	C1–C2 C3–C4	C1–N1/N2 C3–N3/N4	N1–C1–N2 N3–C3–N4
<b>1</b> <sup>[b]</sup>	2.296(1)	1.919(1)	1.376(2)	1.405(2)/1.395(2)	104.4(2)
<b>3</b>	2.322(1)	1.867(4) 1.867(3)	1.424(5) 1.424(4)	1.368(4)/1.364(5) 1.359(4)/1.368(4)	105.7(3) 105.9(3)
<b>5</b> <sup>[b]</sup>	2.419(1)	1.833(3)	1.451(4)	1.354(4)/1.355(4)	107.2(2)
<b>2</b> <sup>[b]</sup>	2.290(1)	1.936(3)	1.369(3)	1.398(3)/1.397(3)	107.3(2)
<b>4</b>	2.330(1)	1.873(2) 1.880(2)	1.427(2) 1.412(2)	1.356(2)/1.364(2) 1.370(2)/1.369(2)	109.67(1) 108.94(1)
<b>6</b>	2.414(1)	1.839(3) 1.822(3)	1.463(4) 1.469(3)	1.335(3)/1.335(4) 1.334(3)/1.334(3)	111.4(2) 111.5(2)

[a] As1–As1'/As1–As2. [b] Molecular structure features crystallographic center of inversion (C).

This can be rationalized as the increase of the formal positive charge on the arsenic atoms of **3** and **4** leads to the  $\pi$ -electron density transfer from the vinylic C=C bond to the arsenic atom.

As expected, a more pronounced trend in the elongation of As1–As1'/As2 and C1–C2/C3–C4 bonds while the contraction of the C2–As1/C4–As2 bond lengths of dications **5** and **6** is observed compared to radical cations **3** and **4**. The As–As bond length of **5** (2.414(4) Å) and **6** (2.414(4) Å) is longer than that of radical cations **3** (2.322(5) Å) and **4** (2.330(1) Å), however it is still shorter compared to an As–As single bond (ca. 2.46 Å).<sup>[10]</sup> Moreover, the C2–As1/C4–As2 bond lengths of **5** (1.836(3) Å) and **6** (av. 1.830(3) Å) are longer than the C=As double bond length of arsalkenes (1.75–1.79 Å).<sup>[11]</sup> The As–As–C angle in **1** (99.0(1)°) and **2** (98.7(1)°) is comparable with that of the corresponding radical cations **3** (av. 99.7(1)°) and **4** (98.0(5)°). The same in dications **5** (95.7(9)°) and **6** (av. 96.3(8)°) is however marginally smaller. These features suggest the presence of a conjugated C<sub>2</sub>As<sub>2</sub>C<sub>2</sub>  $\pi$ -electron system.

Further insights into the electronic structures of **3–6** were obtained by DFT calculations. The optimized geometries of **3–6** at the M06-2X/def2-TZVPP//M06-2X/def2-SVP level of theory (Supporting Information) show good agreement with their solid-state structures. The computed NPA atomic partial charges (Supporting Information, Table T4) indicate that the As<sub>2</sub> fragment in **3** (+0.40e), **4** (+0.47e), **5** (+0.57e), and **6** (0.62e) carries a positive charge, which is higher than that in **1** (+0.27e) and **2** (+0.32e).<sup>[8]</sup> Each of the vinyl (C2/C4) carbon atoms of **3** (–0.54e), **4** (–0.56e), **5** (–0.47e), and **6** (–0.50e) bears a negative, whereas the carbenic carbon (C1/C3) of **3** (+0.42e), **4** (+0.52e), **5** (+0.41e), and **6** (+0.55e) bears a positive charge. The WBIs (Wiberg bond indices) for the As–As bond of **3** (1.25), **4** (1.24), **5** (1.00), and **6** (0.99) as well as for the C2/C4–As bonds of **3** (1.21), **4** (1.19), **5** (1.54), and **6** (1.53) indicate the delocalization of  $\pi$  electrons over the C<sub>2</sub>As<sub>2</sub>C<sub>2</sub> framework. The SOMO (singly occupied molecular orbital) of **3** (Figure 5) and **4** (Supporting Information, Figure F14) is the  $\pi$ -orbital of the As=As bond, whereas the LUMO (lowest unoccupied molecular orbital) is the  $\pi^*$  orbital of the As=As bond. In contrast, the HOMO of **5** (Supporting Information, Figure F15) and **6** (Supporting Information, Figure F16) is the  $\pi$ -type orbital mainly located

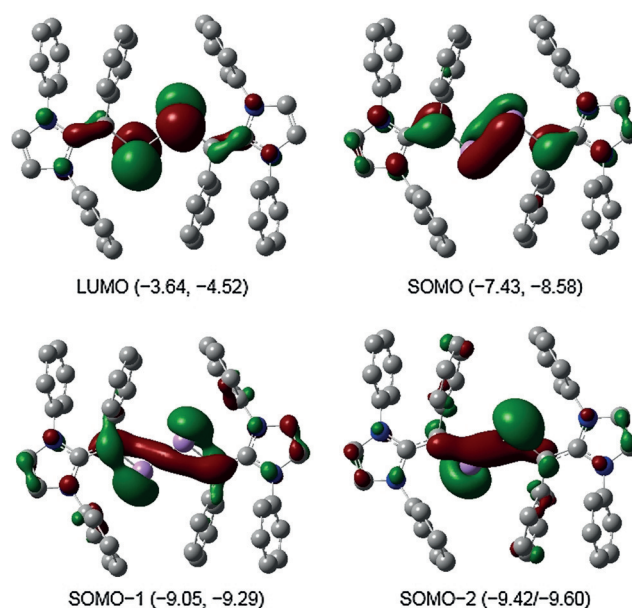


**Figure 5.** Molecular orbitals (isovalue 0.04) of the radical cation **3** calculated at M06-2X/def2-TZVPP//def2-SVP level of theory with energies (eV) for both ( $\alpha$ ,  $\beta$ ) spin states. Hydrogen atoms as well as isopropyl groups are omitted for clarity.

at the C<sub>(Ph)</sub>–As bond. The LUMO of **5** and **6** is the  $\pi^*$  orbital located at the C<sub>2</sub>As<sub>2</sub>C<sub>2</sub> unit. The UV/Vis spectrum of **3** (Supporting Information, Figure F2) and **4** (Supporting Information, Figure F3) each exhibits three main absorption bands, which are red-shifted in comparison to those of **1** and **2**.<sup>[8]</sup> Based on TD-DFT calculations, the band at 822 nm (**3**) and 811 nm (**4**) may be assigned to the SOMO related (S→L and S-1→L) transitions.

The EPR spectra of **3** and **4** were recorded in THF at 9.63 GHz. At 298 K, **3** and **4** exhibit a featureless singlet (Supporting Information, Figures F6 and F7) while at 80 K a broadened septet with poorly resolved hyperfine components was observed because of coupling with two magnetically equivalent <sup>75</sup>As nuclei (Figure 6). These features are similar to those of the radical cation **I** (Figure 1) reported earlier by Robinson and co-workers.<sup>[3a]</sup> The EPR spectra were simulated by using the g values, the hyperfine couplings of each As and *ortho* hydrogen atoms of the phenyl groups, and three linewidth parameters to take into account unresolved hyperfine couplings (Supporting Information, Table T11).

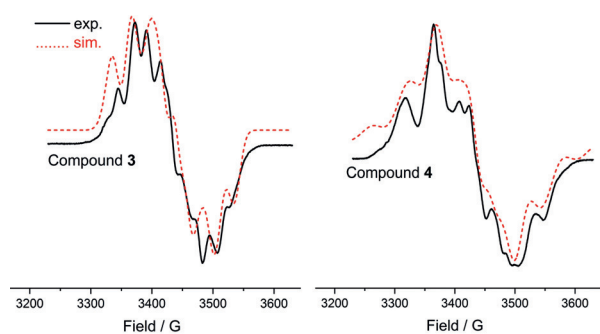


**Figure 6.** X-Band EPR spectra of **3** and **4** at 80 K in THF ( $\nu$  = 9.63 GHz, Mod. Amp. 5G,  $P_{mw}$  = 2 mW).

The calculated Mulliken atomic spin density for **3** and **4** (Figure 7) reveals that the unpaired electron is mainly located at the  $\pi$ -conjugated  $\text{CAs}_2\text{C}$  framework (Supporting Information, Table T10). In **3**, 12% of spin-density is located at each

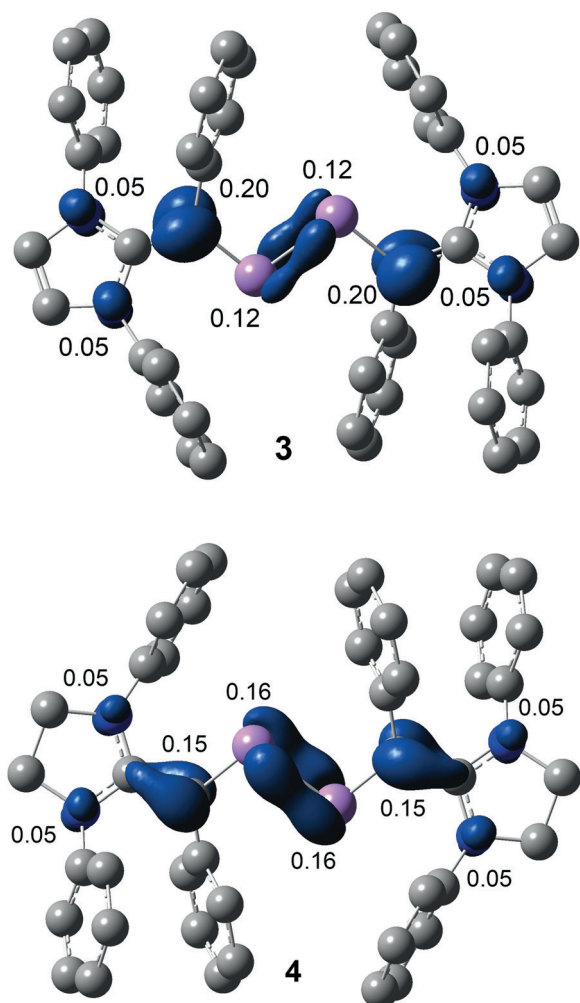


**Figure 7.** Mulliken spin densities calculated at M06-2X/def2-TZVPP//def2-SVP (isovalue 0.04) of **3** and **4**.

of the arsenic atoms whereas the spin density at each of the vinylic carbon atoms is 20%. The spin density at each of the ring nitrogen atoms of **3** and **4** is 5%. Remarkably, the spin density at the original carbene carbon atom is negligible. In comparison with **3**, the spin density at the arsenic atoms (16% each) of **4** is higher compared to that of **3** (12% each). Furthermore, the spin density at the vinylic carbon atoms (15% each) of **4** is lower with respect to that of **3** (20% each). This is most likely due to the puckered (non-planar) structure of 1,3-imidazoline rings of **4** that twist the vinylic  $\text{C}=\text{C}$  bond out of the  $\text{As}=\text{As}$  bond plane, leading to a diminished  $\pi$  conjugation compared to that in **3** featuring planar 1,3-imidazole rings. This is also revealed in the X-ray structures of **3** and **4** (Figures 2 and 3). The  $\text{C}_3\text{N}_2$  ring plane angle of **3** ( $6.53(14)^\circ$ ) is considerable smaller compared with that of **4** ( $83.33(11)^\circ$ ). Similarly, the  $\text{C}2-\text{As}1-\text{As}2-\text{C}4$  torsion angle of  $178.57(14)^\circ$  in **3** is larger than that in **4** ( $163.37(8)^\circ$ ).

In conclusion, the first diarsene radical cations **3** and **4** as well as the dication **5** and **6** have been prepared as crystalline solids. All compounds **3–6** have been characterized by EPR/NMR and UV/vis spectroscopy, and X-ray diffraction and analyzed by computational studies. In accessing **3–6** from **1** and **2**,  $\text{GaCl}_3$  functions as an oxidizing agent and two equivalents of  $\text{GaCl}_3$  are required for one-electron oxidation. The formation of mixed-valence  $\text{Ga}^{\text{I}}/\text{Ga}^{\text{III}}$  compound [ $\text{Ga}(\text{GaCl}_4)$ ] as the main-side product has been shown with  $^{71}\text{Ga}\{\text{H}\}$  NMR spectroscopy. Experimental and theoretical results suggest that the radical cations **3** and **4** are stabilized by the delocalization of unpaired electron over the  $\text{CAs}_2\text{C}$ -unit. DFT calculations reveal that the spin density is mainly located at the arsenic (12% in **3** and 16% in **4** on each As) and vinylic carbon (20% in **3** and 15% in **4** on each C) atoms.

### Acknowledgements

We gratefully acknowledge the support from the Deutsche Forschungsgemeinschaft (DFG). We thank Professor Norbert W. Mitzel for his continuous support. The authors gratefully acknowledge the support by computing time provided by the Paderborn Center for Parallel Computing (PC2).

### Conflict of interest

The authors declare no conflict of interest.

**Keywords:** arsenic · dication · main-group compounds ·  $\pi$  ligands · radicals

**How to cite:** *Angew. Chem. Int. Ed.* **2019**, *58*, 17599–17603  
*Angew. Chem.* **2019**, *131*, 17763–17767

- [1] a) P. P. Power, *Nature* **2010**, *463*, 171–177; b) J. C. Walton, T. R. McFadden, D. P. Curran, *J. Am. Chem. Soc.* **2017**, *139*, 16514–16517; c) R. G. Hicks, *Stable Radicals: Fundamentals and Applied Aspects of Odd-Electron Compounds*, Wiley, Hoboken, **2010**; d) P. P. Power, *Chem. Rev.* **2003**, *103*, 789–809; e) S. Kundu, S. Sinhababu, V. Chandrasekhar, H. W. Roesky, *Chem. Sci.* **2019**, *10*, 4727–4741; f) G. W. Tan, X. P. Wang, *Chin. J. Chem.* **2018**, *36*, 573–586; g) Y. Su, R. Kinjo, *Coord. Chem. Rev.* **2017**, *352*, 346–378; h) M. Soleilhavoup, G. Bertrand, *Acc. Chem. Res.* **2015**, *48*, 256–266; i) C. D. Martin, M. Soleilhavoup, G. Bertrand, *Chem. Sci.* **2013**, *4*, 3020–3030; j) T. Chivers, J. Konu in *Comprehensive Inorganic Chemistry II: From Elements to Applications, Vol. I* (Eds.: J. Reedijk, K. Poeppelmeier), Elsevier, Amsterdam, **2013**, p. 349–373; k) J. Konu, T. Chivers, in *Stable Radicals: Fundamental and Applied Aspects of Odd-Electron Compounds* (Ed.: R. G. Hicks), Wiley, Hoboken, **2010**, p. 381–406; l) K. C. Mondal, S. Roy, H. W. Roesky, *Chem. Soc. Rev.* **2016**, *45*, 1080–1111.
- [2] a) S. L. Hinchley, C. A. Morrison, D. W. H. Rankin, C. L. B. Macdonald, R. J. Wiacek, A. H. Cowley, M. F. Lappert, G. Gundersen, J. A. C. Clyburne, P. P. Power, *Chem. Commun.* **2000**, 2045–2046; b) A. Armstrong, T. Chivers, M. Parvez, R. T. Boeré, *Angew. Chem. Int. Ed.* **2004**, *43*, 502–505; *Angew. Chem.* **2004**, *116*, 508–511; c) S. Ito, M. Kikuchi, M. Yoshifuji, A. J. Arduengo III, T. A. Kononova, L. D. Kispert, *Angew. Chem.*

- Int. Ed.* **2006**, *45*, 4341–4345; *Angew. Chem.* **2006**, *118*, 4447–4451; d) P. Agarwal, N. A. Piro, K. Meyer, P. Müller, C. C. Cummins, *Angew. Chem. Int. Ed.* **2007**, *46*, 3111–3114; *Angew. Chem.* **2007**, *119*, 3171–3174; e) O. Back, B. Donnadiou, M. von Hopffgarten, S. Klein, R. Tonner, G. Frenking, G. Bertrand, *Chem. Sci.* **2011**, *2*, 858–861; f) T. Beweries, R. Kuzora, U. Rosenthal, A. Schulz, A. Villinger, *Angew. Chem. Int. Ed.* **2011**, *50*, 8974–8978; *Angew. Chem.* **2011**, *123*, 9136–9140; g) A. Hinz, A. Schulz, A. Villinger, *Angew. Chem. Int. Ed.* **2015**, *54*, 668–672; *Angew. Chem.* **2015**, *127*, 678–682; h) L. Gu, Y. Zheng, E. Haldón, R. Goddard, E. Bill, W. Thiel, M. Alcarazo, *Angew. Chem. Int. Ed.* **2017**, *56*, 8790–8794; *Angew. Chem.* **2017**, *129*, 8916–8920; i) X. Chen, A. Hinz, J. R. Harmer, Z. Li, *Dalton Trans.* **2019**, *48*, 2549–2553; j) Z. Li, Y. Hou, Y. Li, A. Hinz, J. R. Harmer, C.-Y. Su, G. Bertrand, H. Grützmacher, *Angew. Chem. Int. Ed.* **2018**, *57*, 198–202; *Angew. Chem.* **2018**, *130*, 204–208; k) A. M. Tondreau, Z. Benkő, J. R. Harmer, H. Grützmacher, *Chem. Sci.* **2014**, *5*, 1545–1554; l) O. Back, M. A. Celik, G. Frenking, M. Melaimi, B. Donnadiou, G. Bertrand, *J. Am. Chem. Soc.* **2010**, *132*, 10262–10263; m) O. Back, B. Donnadiou, P. Parameswaran, G. Frenking, G. Bertrand, *Nat. Chem.* **2010**, *2*, 369–373; n) R. Kinjo, B. Donnadiou, G. Bertrand, *Angew. Chem. Int. Ed.* **2010**, *49*, 5930–5933; *Angew. Chem.* **2010**, *122*, 6066–6069; o) Y. Su, X. Zheng, X. Wang, X. Zhang, Y. Sui, X. Wang, *J. Am. Chem. Soc.* **2014**, *136*, 6251–6254; p) A. Brückner, A. Hinz, J. B. Priebe, A. Schulz, A. Villinger, *Angew. Chem. Int. Ed.* **2015**, *54*, 7426–7430; *Angew. Chem.* **2015**, *127*, 7534–7538; q) X. Pan, X. Wang, Z. Zhang, X. Wang, *Dalton Trans.* **2015**, *44*, 15099–15102; r) T. Cantat, F. Biaso, A. Momin, L. Ricard, M. Geoffroy, N. Mézailles, P. Le Floch, *Chem. Commun.* **2008**, 874–876; s) C. Pi, Y. Wang, W. Zheng, L. Wan, H. Wu, L. Weng, L. Wu, Q. Li, P. v. R. Schleyer, *Angew. Chem. Int. Ed.* **2010**, *49*, 1842–1845; *Angew. Chem.* **2010**, *122*, 1886–1889; t) X. Pan, X. Wang, Y. Zhao, Y. Sui, X. Wang, *J. Am. Chem. Soc.* **2014**, *136*, 9834–9837; u) G. Tan, S. Li, S. Chen, Y. Sui, Y. Zhao, X. Wang, *J. Am. Chem. Soc.* **2016**, *138*, 6735–6738; v) S.-s. Asami, S. Ishida, T. Iwamoto, K. Suzuki, M. Yamashita, *Angew. Chem. Int. Ed.* **2017**, *56*, 1658–1662; *Angew. Chem.* **2017**, *129*, 1680–1684; w) M. K. Sharma, D. Rottschäfer, S. Blomeyer, B. Neumann, H.-G. Stammer, M. van Gastel, A. Hinz, R. S. Ghadwal, *Chem. Commun.* **2019**, *55*, 10408–10411.
- [3] a) M. Y. Abraham, Y. Wang, Y. Xie, R. J. Gilliard, P. Wei, B. J. Vaccaro, M. K. Johnson, H. F. Schaefer, P. v. R. Schleyer, G. H. Robinson, *J. Am. Chem. Soc.* **2013**, *135*, 2486–2488; b) S. Demeshko, C. Godemann, R. Kuzora, A. Schulz, A. Villinger, *Angew. Chem. Int. Ed.* **2013**, *52*, 2105–2108; *Angew. Chem.* **2013**, *125*, 2159–2162.
- [4] a) R. Kretschmer, D. A. Ruiz, C. E. Moore, A. L. Rheingold, G. Bertrand, *Angew. Chem. Int. Ed.* **2014**, *53*, 8176–8179; *Angew. Chem.* **2014**, *126*, 8315–8318; b) T. Li, H. Wei, Y. Fang, L. Wang, S. Chen, Z. Zhang, Y. Zhao, G. Tan, X. Wang, *Angew. Chem. Int. Ed.* **2017**, *56*, 632–636; *Angew. Chem.* **2017**, *129*, 647–651; c) T. Sasamori, E. Mieda, N. Nagahora, K. Sato, D. Shiomi, T. Takui, Y. Hosoi, Y. Furukawa, N. Takagi, S. Nagase, et al., *J. Am. Chem. Soc.* **2006**, *128*, 12582–12588.
- [5] a) C. Ganesamoorthy, C. Helling, C. Wölper, W. Frank, E. Bill, G. E. Cutsail, S. Schulz, *Nat. Commun.* **2018**, *9*, 87; b) R. J. Schwamm, J. R. Harmer, M. Lein, C. M. Fitchett, S. Granville, M. P. Coles, *Angew. Chem. Int. Ed.* **2015**, *54*, 10630–10633; *Angew. Chem.* **2015**, *127*, 10776–10779.
- [6] M. Y. Abraham, Y. Wang, Y. Xie, P. Wei, H. F. Schaefer III, P. v. R. Schleyer, G. H. Robinson, *Chem. Eur. J.* **2010**, *16*, 432–435.
- [7] T. Li, G. Tan, C. Cheng, Y. Zhao, L. Zhang, X. Wang, *Chem. Commun.* **2018**, *54*, 1493–1496.
- [8] M. K. Sharma, S. Blomeyer, B. Neumann, H. G. Stammer, R. S. Ghadwal, *Chem. Eur. J.* **2019**, *25*, 8249–8253.
- [9] a) E. S. Schmidt, A. Schier, N. W. Mitzel, H. Schmidbaur, *Z. Naturforsch. B* **2001**, *56*, 337–341; b) H. Schmidbaur, *Angew. Chem. Int. Ed. Engl.* **1985**, *24*, 893–904; *Angew. Chem.* **1985**, *97*, 893–904.
- [10] A. L. Rheingold, P. J. Sullivan, *Organometallics* **1983**, *2*, 327–331.
- [11] a) T. Albers, J. Grobe, D. Le Van, B. Krebs, M. Läge, *Z. Naturforsch. B* **1995**, *50*, 94–100; b) M. Bouslikhane, H. Gornitzka, H. Ranaivonjatovo, J. Escudíe, *Organometallics* **2002**, *21*, 1531–1533; c) D. Ghereg, N. Saffon, J. Escudíe, K. Miqueu, J.-M. Sotiropoulos, *J. Am. Chem. Soc.* **2011**, *133*, 2366–2369.
- [12] CCDC 1939893, 1939894, 1939895, and 1939896 (**3**, **4**, **5**, and **6**) contain the supplementary crystallographic data for this paper. These data are provided free of charge by The Cambridge Crystallographic Data Centre.

Manuscript received: July 22, 2019

Revised manuscript received: September 11, 2019

Accepted manuscript online: September 25, 2019

Version of record online: October 23, 2019